RI 9286

REPORT OF INVESTIGATIONS/1990

Stress Determination in Rock Using the Kaiser Effect

By Michael J. Friedel and Richard E. Thill

1910 ★ 80 YEARS ★ 1990

BUREAU OF MINES

UNITED STATES DEPARTMENT OF THE INTERIOR

Mission: As the Nation's principal conservation agency, the Department of the Interior has responsibility for most of our nationally-owned public lands and natural and cultural resources. This includes fostering wise use of our land and water resources, protecting our fish and wildlife, preserving the environmental and cultural values of our national parks and historical places, and providing for the enjoyment of life through outdoor recreation. The Department assesses our energy and mineral resources and works to assure that their development is in the best interests of all our people. The Department also promotes the goals of the Take Pride in America campaign by encouraging stewardship and citizen responsibility for the public lands and promoting citizen participation in their care. The Department also has a major responsibility for American Indian reservation communities and for people who live in Island Territories under U.S. Administration.

Report of Investigations 9286

Stress Determination in Rock Using the Kaiser Effect

By Michael J. Friedel and Richard E. Thill

UNITED STATES DEPARTMENT OF THE INTERIOR
Manuel Lujan, Jr., Secretary

BUREAU OF MINES
T S Ary, Director

Library of Congress Cataloging in Publication Data:

Friedel, Michael J.
Stress determination in rock using the Kaiser effect / by Michael J. Friedel and Richard E. Thill.

p. cm. – (Report of investigations; 9286)

Bibliography: p. 19

Supt. of Docs. no.: I 28.23:9286.

1. Rocks–Testing. 2. Rock mechanics. 3. Acoustic emission testing. I. Thill, Richard E. II. Title. III. Title: Kaiser effect. IV. Series: Report of investigation (United States. Bureau of Mines); 9286.

TN23.U43 [TA706.5] 622 s–dc20 [622'.28] 89-15871
CIP

CONTENTS

ILLUSTRATIONS

TABLES

UNIT OF MEASURE ABBREVIATIONS USED IN THIS REPORT

°C	degree Celsius	lb	pound
cm	centimeter	MHz	megahertz
dB	decibel	MPa	megapascal
kg m^2/s	kilogram-meter squared per second	pct	percent
kHz	kilohertz	psi	pound per square inch
kN	kilonewton	s	second

STRESS DETERMINATION IN ROCK USING THE KAISER EFFECT

By Michael J. Friedel[1] and Richard E. Thill[2]

ABSTRACT

The U.S. Bureau of Mines investigated acoustic emission (AE) and the Kaiser effect in six types of rock: St. Cloud gray granodiorite, Barre granite, Dresser basalt, Salem limestone, Berea sandstone, and a volcanic tuff. AE signatures were used for interpreting the rock deformation stage and for indicating mechanisms of failure in uniaxial compression. The research demonstrated the advantages of using the volumetric stress-strain curve, as opposed to the more conventional uniaxial curve, for correlating AE response signatures with deformation stages and fracture processes in the rock. Standardized experimental procedures were used for the AE monitoring. The Kaiser effect was shown to be capable of determining prestress levels to within a few percentage points in uniaxial compression tests. Also, prestress memory was shown to be retained in the rock for periods of up to at least 5 months, the maximum period of testing. The Kaiser effect AE technology holds promise for providing a comparatively inexpensive and less complex method for examining stress history in rock. However, since the confining stress has a pronounced influence on the Kaiser effect, it must be considered in developing technology for determining peak field stresses based on the Kaiser effect.

[1]Geophysicist.
[2]Supervisory geophysicist.
Twin Cities Research Center, U.S. Bureau of Mines, Minneapolis, MN.

INTRODUCTION

Knowledge of the state of stress in a rock mass is of utmost concern in many mining applications. Reliable evaluations of in situ stress are needed for mine design, particularly for evaluating the stability of mine structures to prevent failure or collapse of underground mine openings. In situ stress is one of the necessary parameters for input into models for mine design and stability analyses. The state of stress often is a controlling factor in the economics of mining operations, entering into the determinations of the size and spacing of openings, extraction rates and ratios, and the type and amount of support required.

In in situ mining operations, the state of stress controls the permeability of fluids through fracture systems and, therefore, to a large extent, the recovery of ore from the zones of mineralization. Moreover, the stress state is of paramount importance in the creation of fractures, either by hydraulic or explosive means, to enhance permeability for the recovery of minerals.

Although numerous approaches have been developed to determine in situ stress, none are universally applicable in rock and all suffer from deficiencies and limitations (*1*).[3] Technology is particularly deficient for determining the stress state at depth in remote regions that are inaccessible from boreholes or mine workings, or for corrosive environments, such as may be encountered in in situ leaching or waste disposal. Two major problems with current technology are (1) the nature of tools and methods of access to the zone of stress determination in the rock, e.g., borehole deformation or flat jack tools, may alter the stress state in the process of measurement and thereby may yield questionable results, and (2) current methods determine state of stress at a point, whereas an integrated or averaged value of the rock mass stress state may be more appropriate for use in mining applications. Other shortcomings of current stress determination methods are that they usually are expensive and time consuming and have limited capabilities, if any at all, for stress determinations in weak, fractured, or anisotropic rocks. Continued research and development of new and improved technology is necessary for more accurate and reliable determinations of in situ stress in difficult mining situations.

A novel approach for determining in situ stress at depth and in remote regions or in corrosive and hostile environments is to use secondary effects of stress such as can be measured by geophysical methods. A recent report of the National Research Council, giving an evaluation of in situ stress measurement technology in rock (*2*), emphasizes that "geophysical methods most likely will be the only tools for evaluating stress conditions at great depths, or at sites where drilling is limited or precluded by economic or possibly design requirements, or where the installation of measuring devices can be expected to alter the ambient stress field." One of the more promising of the geophysical techniques for determining the state of stress in rock is the use of the so-called Kaiser effect, obtained during measurements of acoustic emission (AE) in stressed rock. Kaiser (*3*) observed that AE activity exhibited an irreversible effect upon unloading and reloading metal specimens tested in uniaxial tension. Upon reloading a specimen, Kaiser noted that AE activity was substantially quiet until the stress level of the previous maximum applied stress was exceeded. This phenomenon, termed the "Kaiser effect," suggests that previous maximum stress levels might be detected by stressing a rock to the point where there is a substantial rate of change in AE activity. Although the Kaiser effect has been well established in metals, only limited research has been conducted in a few types of rocks. Most notable is the recent work of the Japanese (*4-8*), Hardy (*9-10*) at the Pennsylvania State University, and Holcomb (*11-13*) at the Sandia National Laboratories. Little research, however, has been directed toward devising methods to apply this stress determination technique to practical mining situations and problems.

The purposes of this investigation are (1) to verify the applicability of the Kaiser effect for determining previous stress history in several types of rock common to mining, (2) to compare stages of AE behavior or AE signatures in different rock with those previously defined by Mogi (*7*) or Boyce (*14*), and (3) to relate the AE signature to the deformation response and failure mechanisms of rock. The results presented in this report represent the first phase of research by the U.S. Bureau of Mines on utilizing the Kaiser effect for in situ stress and stress change determinations in mining applications. This work is in support of the Bureau's mission to enhance mine safety, by remotely assessing the state of in situ stress.

[3]Italic numbers in parentheses refer to items in the list of references at the end of this report.

EXPERIMENTAL PROCEDURES

Experimental procedures were implemented (1) to provide a more standardized approach in testing procedures, (2) to permit discrimination between AE signals and electromagnetic noise, (3) to improve the signal-to-noise ratio, and (4) to graphically portray AE results to facilitate data interpretation. Several types of crystalline and sedimentary rock were selected for the experimentation to represent a variety of types of rock encountered in mining. These included St. Cloud gray granodiorite, Barre granite, Dresser basalt, Nevada volcanic tuff, Berea sandstone, and Salem limestone. Several of the rocks were selected because they were part of a standardized suite of rocks for which much property and petrographic data had been determined (*15*).

Cylindrical cores 2.54 cm in diameter by 5.08 cm long were taken in a single direction in rock blocks to prevent variation in results due to anisotropy. Specimen dimensions and surface end finishing conformed to guidelines for uniaxial testing recommended by the American Society for Testing and Materials (*16*) and the International Society of Rock Mechanics (*17*). Precisely sectioning and polishing specimen ends minimized the potential for noise generation due to platen seating at the specimen interface or other frictional movements due to end-surface irregularities. Rock cylinders were then weighed for initial density determinations and, subsequently, preconditioned in a vacuum oven at a moderately elevated temperature of 100° C to remove moisture and obtain a standardized dry testing environment for the uniaxial loading experiments. Specimens were stored in a desiccator until the time of testing.

MECHANICAL TESTING PROCEDURES

Unconfined uniaxial compression tests were conducted using a closed-loop, servocontrolled materials-testing machine, having 250,000 lb (1,096 kN) load capacity. Specimens were preloaded to levels of about 7 MPa for the crystalline rocks and 0.5 MPa for the tuff and sedimentary rocks to initially seat the platens and close the loop for automated servocontrol. Rocks were loaded at strain rates ranging between 2×10^{-4} and 2×10^{-6} per second, based on recommendations in earlier work (*14*). Triaxial data are from the reanalyzed information presented in an earlier study in which test procedures were similar to those used in the uniaxial tests (*18*).

AE sensing and processing was done with a wideband (100 kHz to 1 MHz) piezoelectric transducer and an AE analyzer, modified to operate in a frequency range down to 100 kHz. The AE analyzer was a real-time data acquisition system with capabilities for storage and parametric display of incoming signals. The AE transducer was attached to an aluminum contact piece that was shaped to the curvature of the test specimen. This increased the contact area between the transducer and specimen, allowing for increased energy transmission into the detector. Aluminum has an acoustic impedance of 1.7 kg m^2/s, intermediate between that of the piezoelectric transducer and that of most rock. Hence, it was an appropriate choice for providing good transmission of energy from the rock to the detector transducer. The aluminum front piece, moreover, acted as a wear plate, protecting the front electrode of the transducer. Silicone grease was used as a couplant between the aluminum front piece and the specimen surface to compensate for any microscale roughness or asperities in the contact surfaces. This again provided for optimum energy transmission at the transducer-rock interface.

The schematic for the AE detection system is given in figure 1. An elastic wave generated as AE in stressed rock is converted to an electrical signal by the transducer. This electrical signal is then transferred via coaxial cable to a 60-dB preamplifier and into the AE analyzer through an adjustable-gain, linear amplifier, which provides up to 21 dB additional gain in 3-dB increments. The analyzer is equipped with two floppy disk drives for the storage of AE data. Output from the AE analyzer can be displayed in terms of AE accumulative counts or rate for events, counts, or energy (fig. 2). External parametric input to the analyzer permits the simultaneous input and plotting of load (stress) or deformation (strain) data as a function of the AE response. Sampling rate for the parametric digital sampling was 1,000 samples per second. A digital oscilloscope is used for waveform capture and transfer for analysis to a computer.

Signal noise arose from two main sources: electromagnetic disturbances and mechanical vibrations. "Noise" refers to any random or persistent disturbance that obscures or reduces the clarity of received AE signals. The electromagnetic noise comprises both steady-state background noise and spurious in-line electrical transients. Electromagnetic noise was reduced as much as possible by grounding and shielding electrical components and using coaxial shielded cable for transmission lines. Mechanical vibrations predominantly occurred in a low-frequency range. These and 60-Hz or other low-frequency electromagnetic noise were effectively eliminated by using a low-frequency cutoff analog filter to discriminate against frequencies below 100 kHz. The appropriate amplification level to provide the maximum amplification of AE signals, yet discriminate against transient and background noise, was determined by placing the detector transducer on the platen head with all electrical components and servovalves of the mechanical testing system turned on. This presented the situation with greatest noise generation. Trigger levels of the AE analyzer then were set at their lowest point to pass all noise transients, and amplification was reduced in 3-dB increments from the highest amplification setting of 81 dB, where noise saturation occurred, until background counts per event were less than about 5. The optimum gain setting was found to be 66 dB. To further discriminate AE signals from background noise during the tests, analyzer threshold trigger levels were raised above the background noise level. To discriminate AE signals from spurious noise, only those AE events having 5 or more counts (in excess of the threshold trigger level) and exceeding 100 kHz in frequency were used in the data analysis.

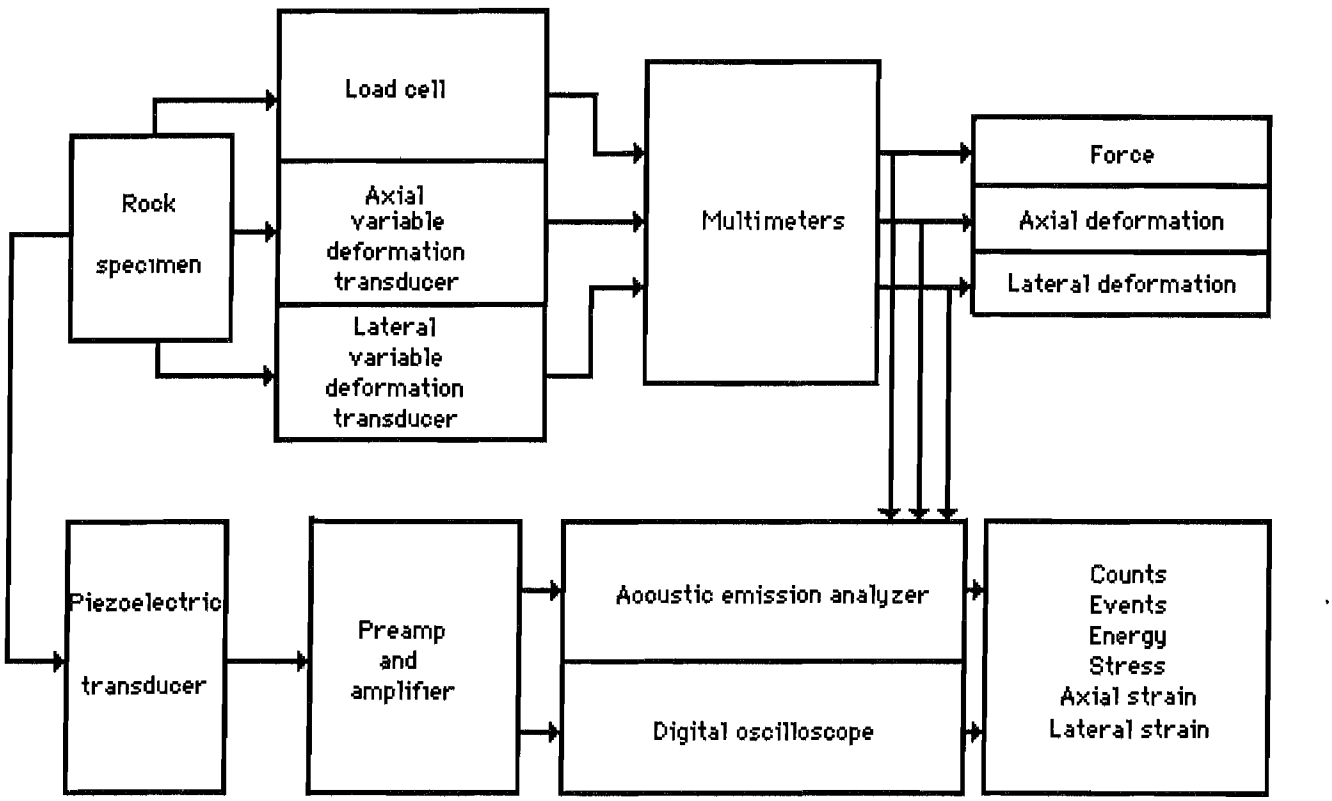

Figure 1.–Acoustic emission test system.

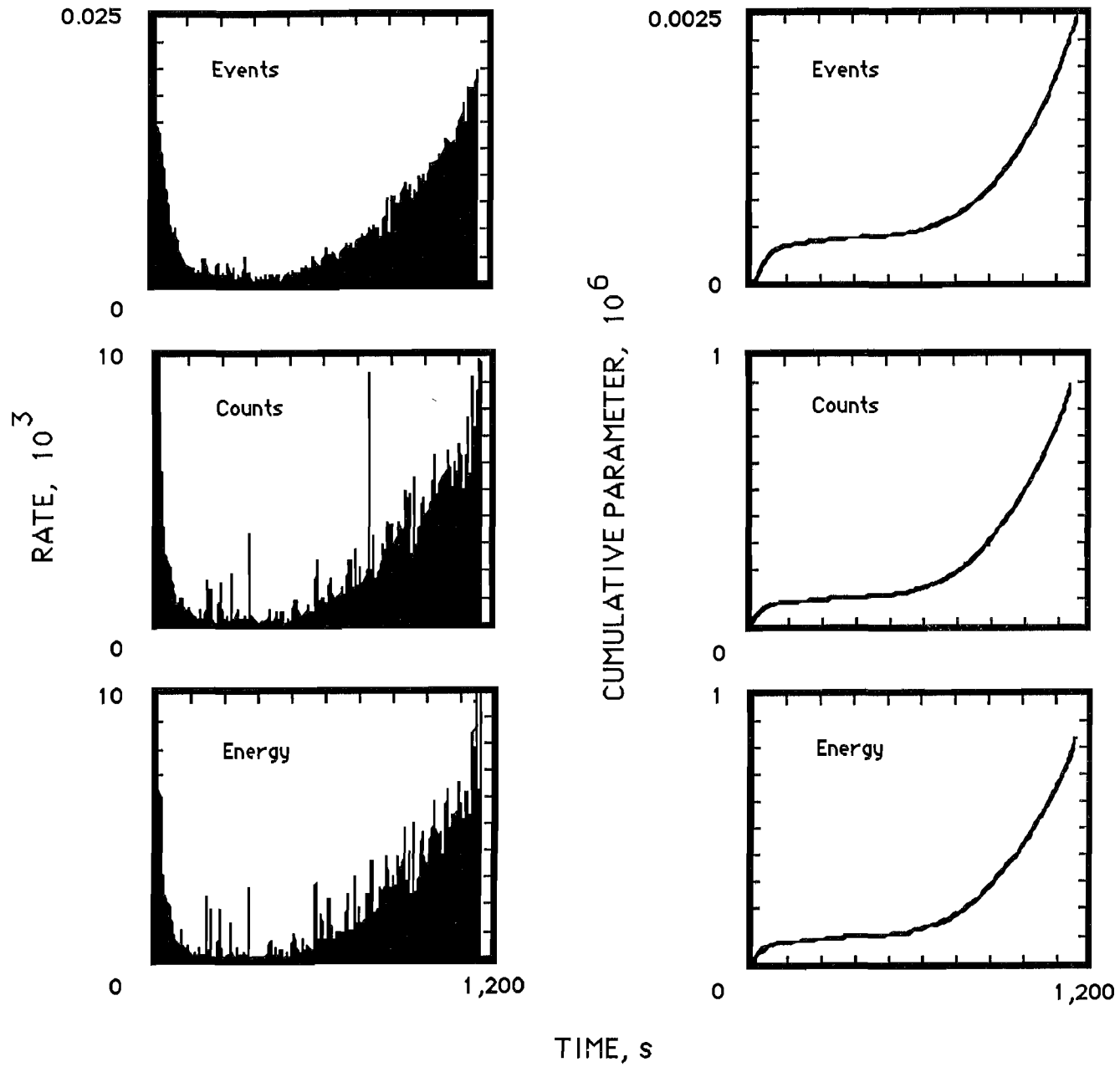

Figure 2. –Examples of parametric output for St. Cloud gray granodiorite sample loaded to rupture under uniaxial compression. Acoustic emission data were processed over a 1-ms time interval.

ACOUSTIC EMISSION SIGNATURES

Typical AE response curves for cumulative emission in the six rock types as a function of uniaxial unconfined compressive stress are given in figure 3. Several types of signatures or patterns are recognized in the AE response curves. One type of signature is defined by the overall shape of the AE response curve, sometimes referred to as the "Mogi" type of curve. This type of signature relates to the generalized regions of deformational response and the fracture process in elastic-plastic materials (fig. 4).

Mogi (*7*) classified the commonality in shapes of cumulative AE response into four distinct regions. These have been associated with the Bieniawski model of deformation response or fracture processes (fig. 4) in rocks (*14*). In region I (A-B), crack closure and/or compaction occurs, resulting in a positive increasing slope in the cumulative AE curve. In region II (B-C), the rock undergoes semilinear elastic deformation, with a correspondingly low, nearly constant rate of AE. Hence, the slope of the cumulative AE curve in this region is low and nearly constant. Region III (C-D) is typified by the onset of fracturing and stable crack growth and is represented by an abrupt increase in AE activity (the Kaiser effect) with sharply increasing slope. Region IV (D-F) relates to critical energy release and unstable fracture propagation that extends to rupture in brittle materials or continued permanent deformation in elastoplastic or plastic materials by strain-hardening or strain-softening processes. Region IV is typified in the AE response curve by high rates of AE with steeply increasing slope. Thus, slope changes and inflection points of the AE response curve can be used for interpretation of the general regions of rock deformation under compressive loading conditions. These deformation regions can be interpreted even more precisely using combined AE and elastic wave velocity (*18*).

In Bureau experiments, researchers observed that the shape of the AE curves, relating to the various stages of deformation (Mogi signature), was similar whether cumulative emission was measured as a function of time, stress, or strain (fig. 5). Curve shapes, moreover, also were similar if different AE parameters, such as rate, energy, or cumulative events were used (fig. 2). Hence, signature analysis of these different forms of output would provide generally similar results when interpreted broadly in terms of the different stages of rock deformation or fracture.

Boyce (*14*) recognized that there are several variations of the Mogi pattern and classified four types of signature responses for cumulative AE in rock under uniaxial compression (fig. 6). In some rocks, some of the stages of the Mogi model appear to be missing or undetectable. The type I signature with four distinct slope changes was classified as the "Mogi" signature. The type II signature was designated "unstable," relating to the absence of the third-phase segment (C-D) of the Mogi model. This implies that the material changes directly from linear elastic behavior into unstable crack propagation, without a phase of stable crack growth. The type III signature was designated "dense" by Boyce, referring to the absence of the first phase (segment A-B) of the Mogi model. The type III model implies that this type of rock is intact and dense, and therefore lacks a crack closure-consolidation phase in the initial stages of uniaxial stress application. The type IV signature lacks both the first and third phases of the Mogi model and is designated "dense, unstable," incorporating aspects of both type II and type III behavior.

In applying AE signature classification to the rock tested, the Bureau found that all segments (slope changes) of the Mogi type of signature were present to some extent in each type of rock (e.g., fig. 3). For some of the rocks, however, it appeared that certain slope segments of the Mogi type of curve were almost absent. These closely resembled the Boyce types of signatures, e.g., the Berea sandstone curve appeared almost linear in the CD-DF segment and therefore could be classified as "type II-unstable" in Boyce's signature classification scheme. Similarly, the St. Cloud gray granodiorite curve appeared to closely resemble the "type III-dense" signature.

Several problems were noted, however, in attempting to use the Boyce classification. Appearance of the curve shape, and therefore its signature classification, was affected by changes in the settings of the data acquisition system or even the scale selected for plotting. Setting the trigger threshold higher or lower or changing the sampling rate, e.g., could cause greater or less development of certain segments of the curve. For instance, by changing the sampling rate interval or the amplitude threshold, or by applying an initial preload to the sample, the shape of the AE curve could be changed to reduce or eliminate the A-B and C-D segments of the signature. These problems indicate there is need for standardization of the data acquisition and plotting parameters for use of the Boyce classification system.

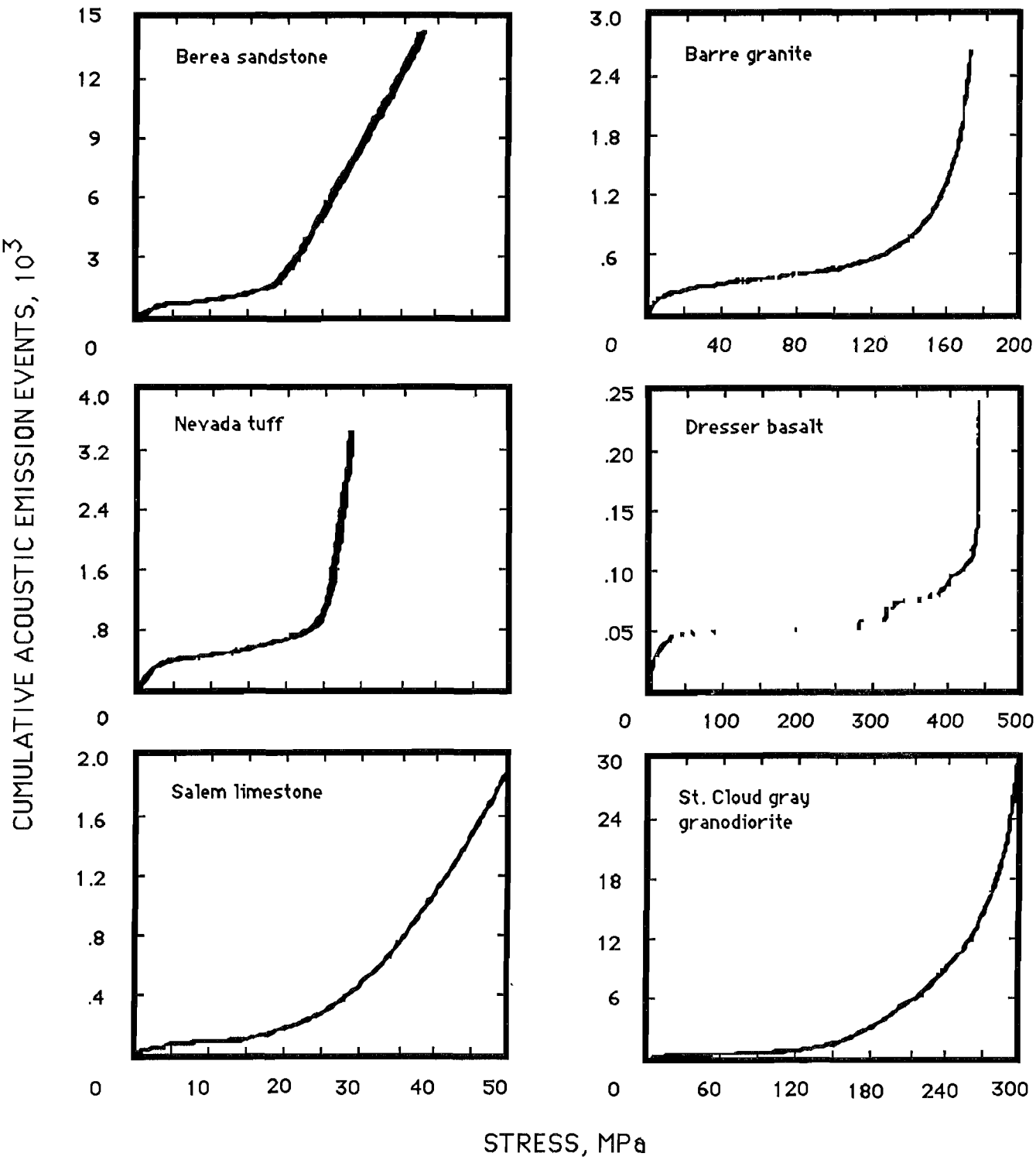

Figure 3.–Cumulative acoustic emission events as a function of stress for various sedimentary and igneous rocks loaded under uniaxial compression.

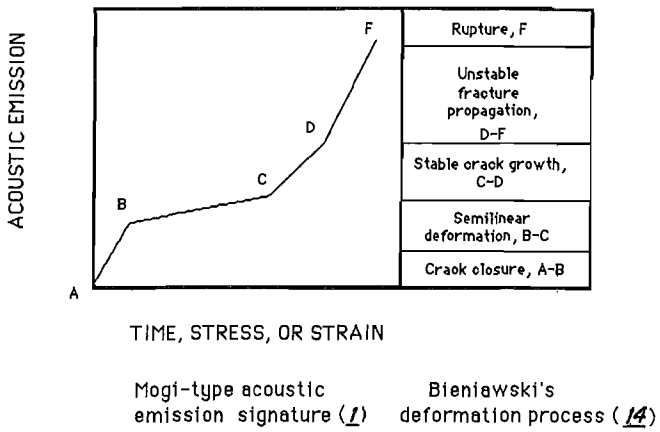

Figure 4.–Acoustic emission response characteristics associated with the five regions of deformational behavior, or the fracture process.

In addition to the generalized shape of the AE response curve, which was shown to be closely related to the deformation stages of rock at different levels of stress and strain, other diagnostic AE signatures or patterns exist that appear to be associated with the internal rock structure and mechanisms of failure. These patterns arise in the more detailed AE response within each deformation region and also from the acoustic waveform response associated with each event. Each type or family of rock appears, therefore, to have a distinct pattern of AE that distinguishes it from others (e.g., fig. 3). Some rocks are very noisy (high AE) in the early, low-stress region of deformation, whereas others may have few AE events in this region. Some have low cumulative AE into the very high-stress region and then suddenly burst with high rates of AE close to the rupture stage (e.g., Dresser basalt). Other rocks (e.g., Berea sandstone or Salem limestone) may have nearly constant rates of AE over wide ranges of stress preceding failure. These individualized signatures for each type of rock appear mainly to be related to rock fabric, particularly crack defects, the loading conditions, and the mechanisms of failure. The association of the AE signature with rock fabric and the microstructural mechanisms of deformation and failure are not well established. However, in rock exhibiting brittle behavior, microcracks have been shown to play a dominate role in the types and amount of AE generated in deformation regions I, III, and IV (Thill, *18*; Scholz, *19-20*; Brace, 21; Montoto, *22*). Lord and Koerner (*23*) emphasize that a greater concerted effort needs to be made for identifying the source mechanisms of AE and for distinguishing between those mechanisms associated with continuous emissions and those associated with burst emissions.

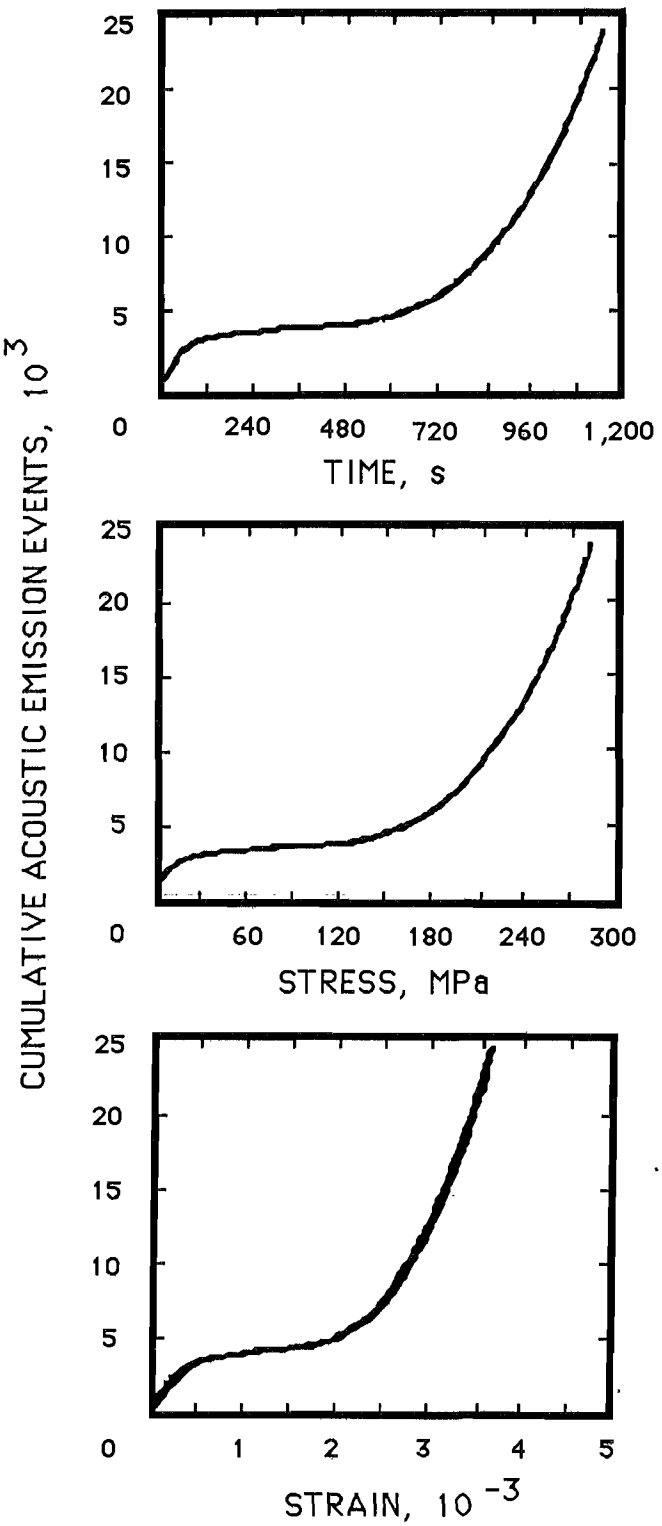

Figure 5.–Cumulative acoustic emission events as a function of time, stress, and strain for St. Cloud gray granodiorite sample loaded under uniaxial compression.

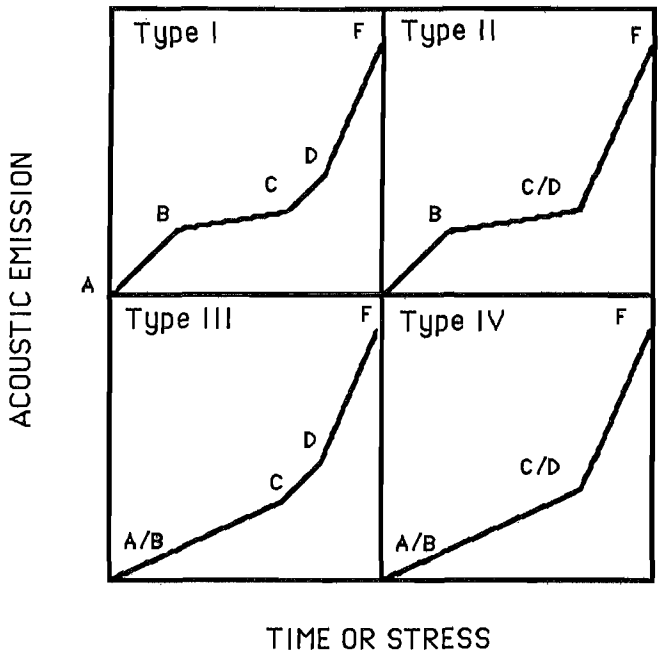

Figure 6.–Boyce signature classification based on shape of cumulative acoustic emission response curve in different types of rock (*14*). Classifications: type I, Mogi-type curve; type II, unstable; type III, dense; type IV, dense unstable.

Because AE signatures or patterns are shown to be diagnostic of stress-strain behavior, the deformation process, and the mechanisms of failure in rock, computerized pattern recognition technology presents a viable approach for interpreting stress and deformation characteristics or mechanisms of failure in stressed rock. The pattern recognition approach requires training input from the AE response curves or from captured AE waveforms and the use of artificial intelligence to obtain predictive capabilities on the stage of stress or deformation and the failure mechanisms in rock (fig. 7). Some use of pattern recognition technology has already been reported in Canadian research (*24*) for determining stress level in rock and recognizing impending failure.

Several volumetric stress-strain tests were conducted to confirm the correlation of cumulative AE response to volumetric stress-strain behavior and the deformation processes (fig. 8). For brittle rock, initial nonlinearity in the volumetric stress-strain curve is associated with crack closure and compaction. The initial deviation of the volumetric curve from projected linear volumetric compression marks the onset of volume dilatation associated with the formation of cracks. The transition from stable to unstable crack propagation occurs at the reversal in the volumetric stress-strain curve from positive to negative slope.

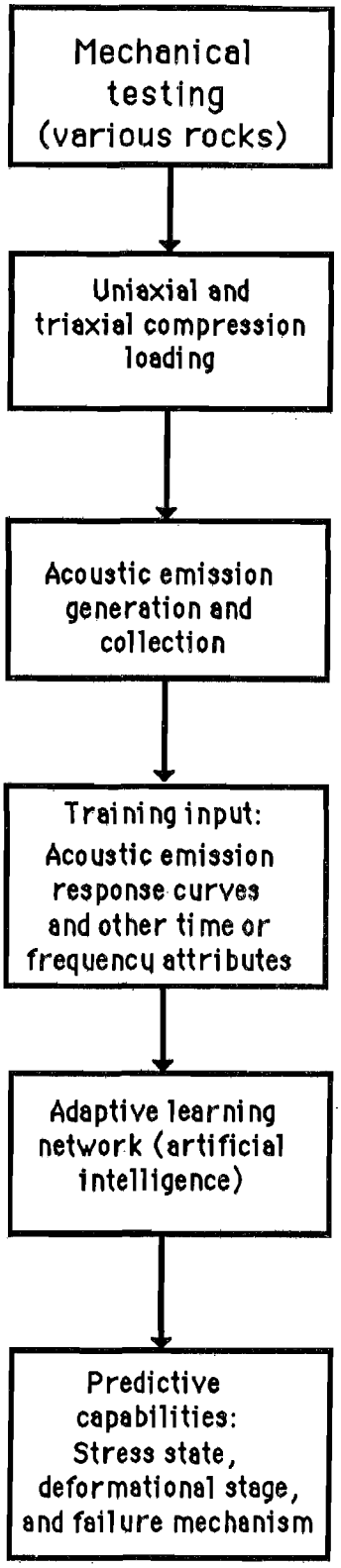

Figure 7.–Acoustic emission pattern recognition.

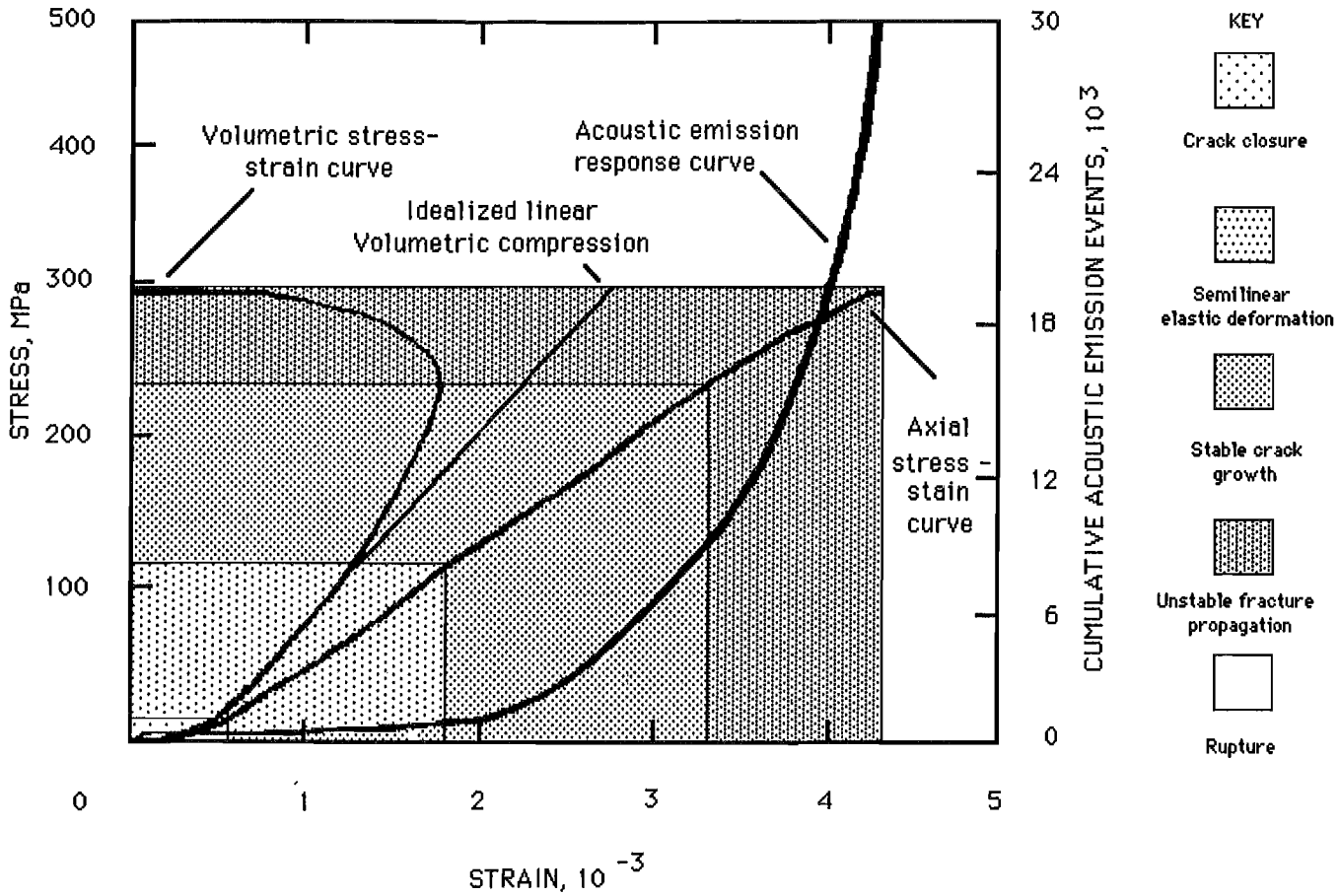

Figure 8.–Cumulative acoustic emission events as a function of both axial and volumetric stress-strain for typical St. Cloud gray granodiorite sample loaded under uniaxial compression.

These volumetric stress-strain stages coincide with slope changes in the cumulative AE response curve and therefore assist in the interpretation of AE response in AE field monitoring situations. Currently, it is common practice to plot AE response as a function of the axial stress-strain behavior. The onset of dilatation and transition from stable to unstable fracture propagation, however, generally are not as apparent from the axial stress-strain curve. Hence, for interpretation of AE in terms of the deformation processes in rock, it is recommended that AE be plotted as a function of the volumetric rather than the axial stress-strain curve.

KAISER EFFECT

Typical AE rate response for the first cycle of uniaxial unconfined loading for Salem limestone (fig. 9) gives clear definition of the deformation regions of crack closure, linear elastic deformation, stable fracture propagation, unstable fracture propagation, and failure (or postpeak behavior). The Kaiser effect, i.e., the point at which AE rate begins to increase above the background rate observed in the linear elastic region, is picked at a stress level of about 19 MPa. This apparently represents the locked-in peak stress to which the rock had been subjected. Peak stresses similarly determined for the six types of rocks in this study are given in table 1. These results support those of Holcomb (*11-12*), Hardy (*9-10*), and Kurita and Fujii (*6*), who established that induced prestresses could reasonably be determined by the Kaiser effect. Holcomb's experiments (*12*) also indicated that even explosion-induced, dynamic peak stresses might be estimated using the Kaiser effect, if the yield strength of the rock has not been exceeded. Kanagawa (*25*) further made comparisons with the conventional overcoring in situ stress determination method and found that the Kaiser effect method for determining stress in rock cores compared favorably with

Table 1.–Peak stress history as determined by Kaiser effect

Rock classification	Name	Previous peak stress, MPa[1]	Range, MPa
Sedimentary . .	Salem limestone . .	19	±2
Do	Berea sandstone . .	31	±1
Igneous	Nevada tuff	33	±2
Do	St. Cloud gray granodiorite.	115	±5
Do	Barre granite	136	±4
Do	Dresser basalt	263	±12

[1]Statistical mean of 5 samples.

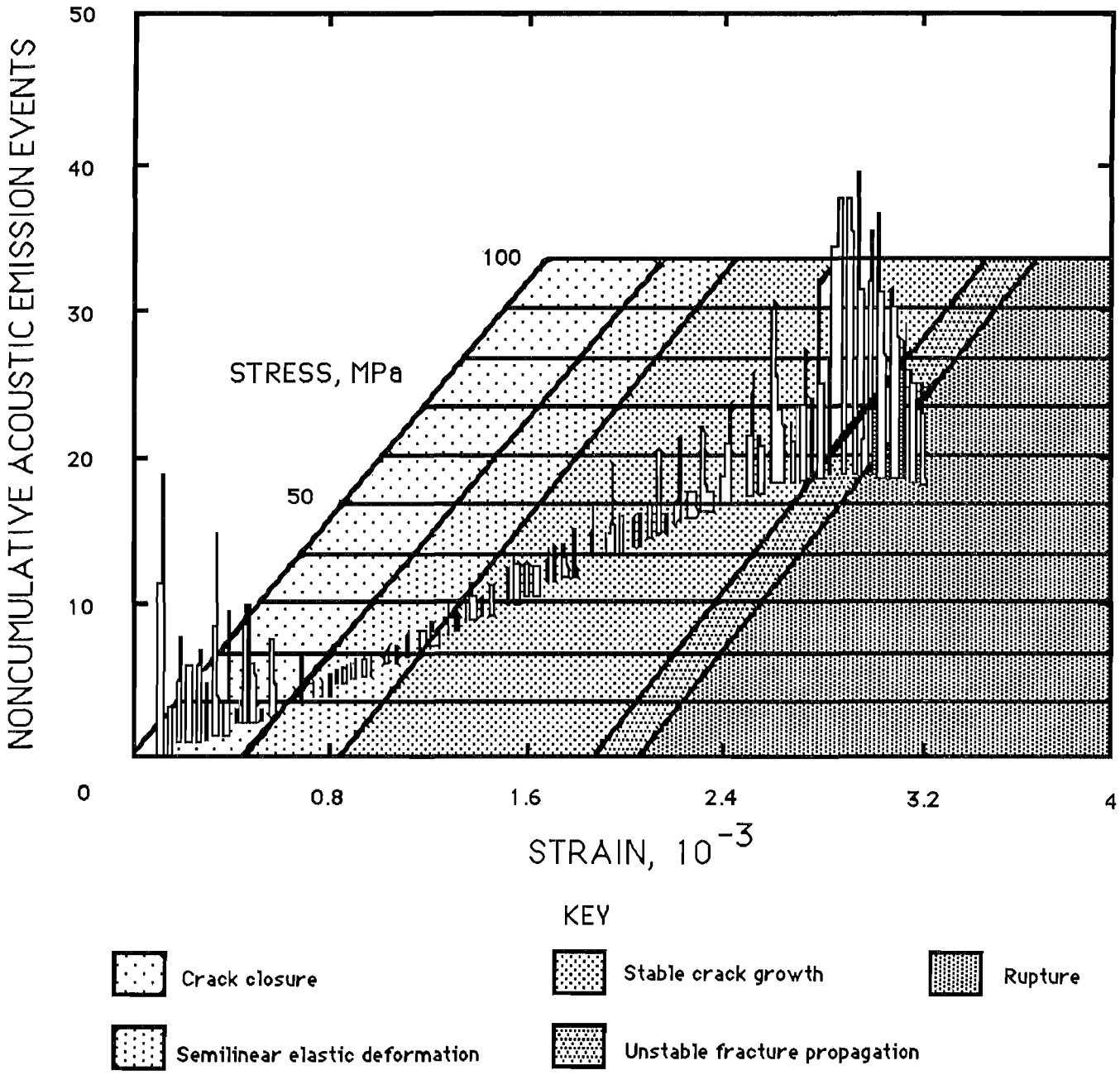

Figure 9.–Acoustic emission response and its correlation to brittle deformation criteria for typical Salem limestone sample.

in situ stress determinations made by an overcoring method for a mudstone, but the results of the two methods varied for a granite. The reason for the difference in the latter, however, was explained by the fact that the overcoring technique was used after removal of considerable overburden in the granite, whereas the Kaiser effect determination seemed to reflect stresses in situ before the removal of overburden.

In the Kaiser effect method, the first loading cycle often produces noise associated with crack closure or compaction that can sometimes obscure the Kaiser effect. This noise in the first cycle of loading, however, can be suppressed by subsequent unloading-reloading cycles at stress levels below the Kaiser effect (fig. 10), thereby making the onset of an increase in AE rate associated with the Kaiser effect more pronounced. Most noise is reduced by the second cycle, with only slight improvement in subsequent cycles.

Examples of the capability of the Kaiser effect to determine prestressed levels are given for St. Cloud gray granodiorite (fig. 11) and Salem limestone (fig. 12). In both cases, cumulative AE was plotted directly as a function of the axial stress-strain curve. The first loading cycle (A) prestressed the sample to a known stress level. The stress was held constant at this level until creep occurred. The sample was then unloaded (stress path B) and reloaded along stress path C while measuring cumulative AE (curve D). The Kaiser effect stress is readily determined from the point of intercept on the stress-strain curve associated with the onset in rate change in the AE curve.

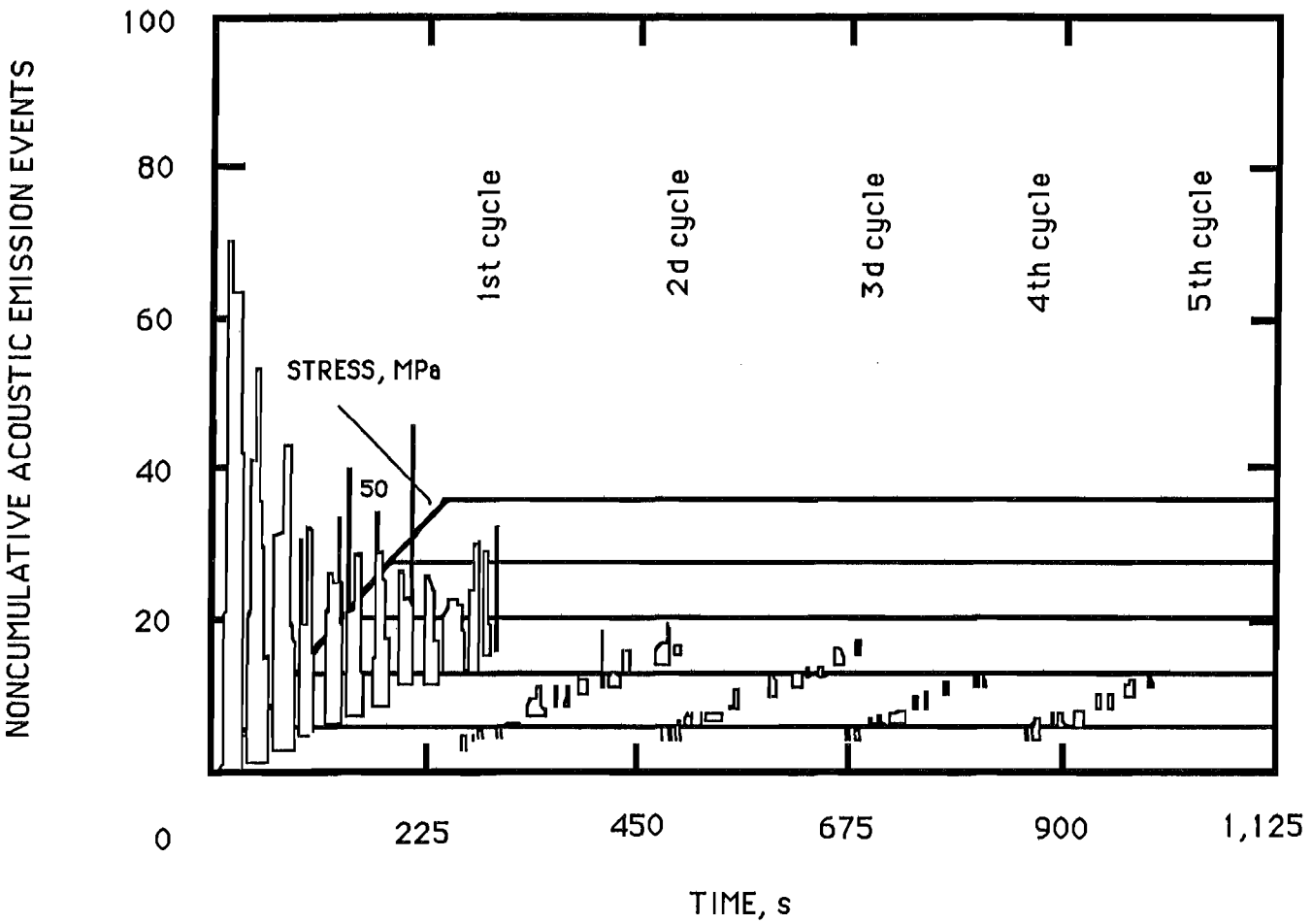

Figure 10.–Reduction of acoustic emission events associated with crack closure. Subsequent cycling shows an advantage to preloading the rock into the linear elastic range to enhance Kaiser effect.

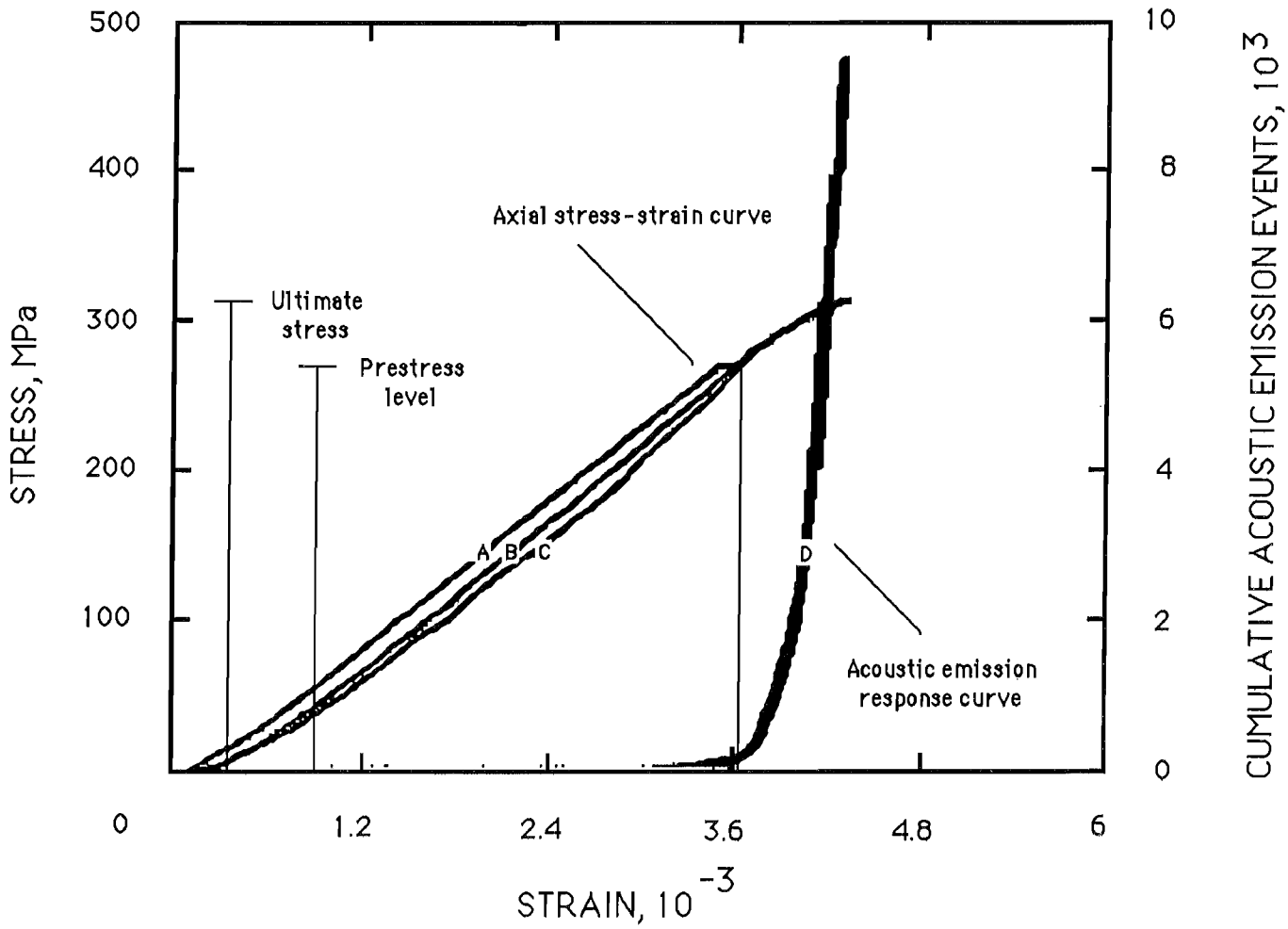

Figure 11.–Cumulative acoustic emission events as a function of stress-strain response for St. Cloud gray granodiorite under uniaxial compression. Curve A-C represents initial stress-strain path taken; curve B is subsequent stress-strain path taken to failure. Curve D depicts cumulative acoustic emission response during the subsequent stress-strain cycle.

Uniaxial tests conducted in several rocks at different levels of prestress indicated that the Kaiser effect was operable within the region between the previous peak stress and unstable yielding of the sample. Table 2 gives several stress determinations of prestress levels for limestone and granodiorite. Stress levels could be reestablished to within a few percentage points. At stress levels sufficient to cause unstable yielding, however, stress relaxation can occur and the Kaiser effect may be absent or indicative of residual rather than peak stress. This is a subject for follow-on studies. In research by Holcomb and Martin (*12*), a Kaiser effect could not be established in a test specimen of tuff that was prestressed near the location of a nuclear explosion at a Nevada test site. Instead of an

Table 2.–Kaiser effect detection of prestress levels in Salem limestone and St. Cloud gray granodiorite

Rock	Kaiser effect stress, MPa	Previous applied stress, MPa	Difference, MPa
Salem	37.5	39.0	-1.5
limestone.	47.4	47.0	+.4
	58.2	57.0	+1.2
St. Cloud	132.0	136.0	-4.0
granodiorite.	143.0	142.0	+1.0
	285.0	278.0	+7.0

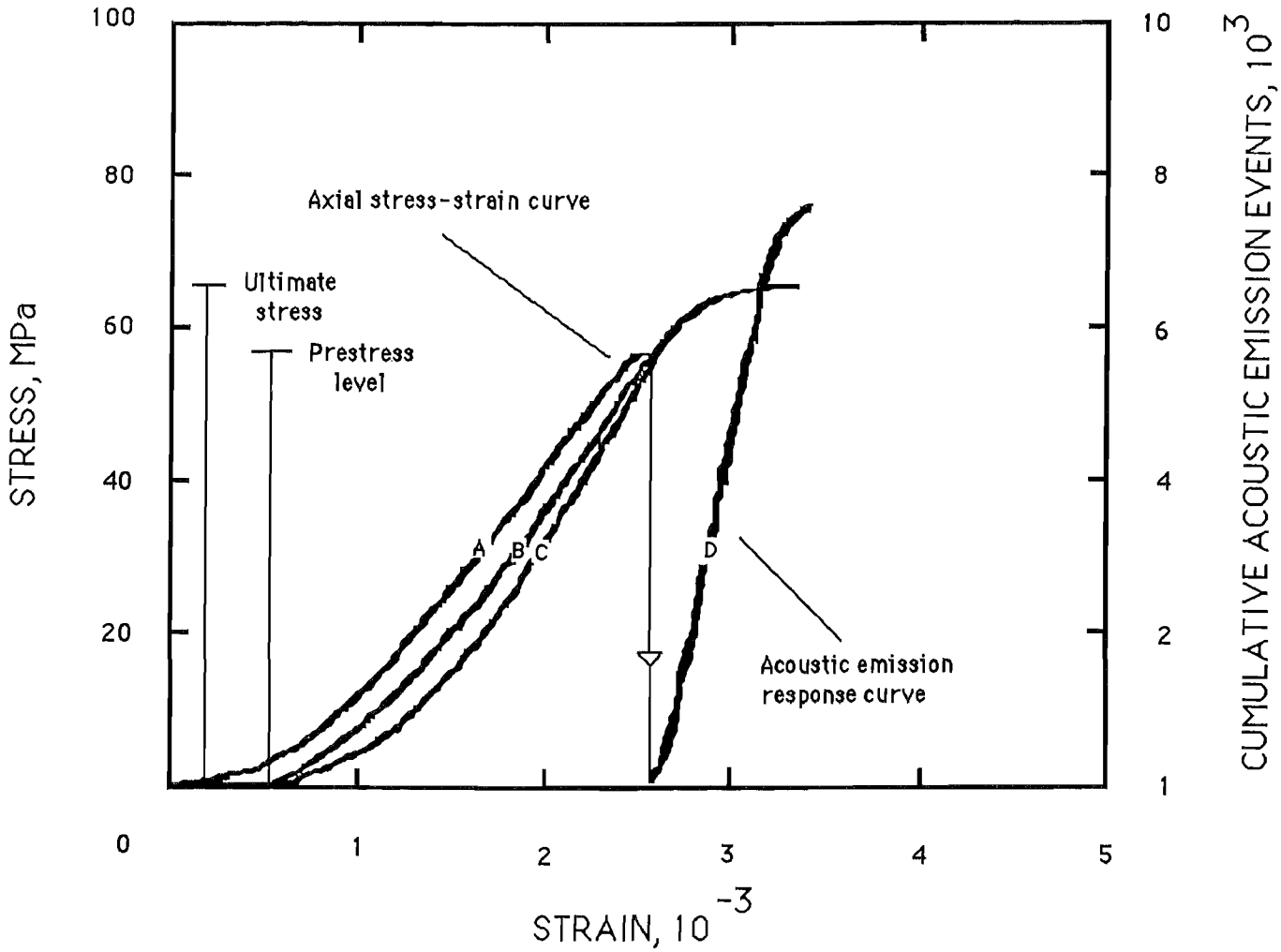

Figure 12.–Cumulative acoustic emission events as a function of stress-strain response for Salem limestone under uniaxial compression. Curve A-C represents initial stress-strain path taken; curve B is subsequent stress-strain path taken to failure. Curve D depicts cumulative acoustic emission response during the subsequent stress-strain cycle.

increase in AE with increasing uniaxial stress, the number of AE events per stress increment stayed relatively constant during loading and tended to decrease at higher stresses. It was concluded that the sample had been stressed to "yield" by the explosion and therefore was incapable of indicating the previous maximum stress to which it had been subjected. The above results suggest that an upper limit is placed on the useful range of the Kaiser effect and further indicate that weak rock may not be suitable for reestablishing regional peak stress history by this method if peak stresses have exceeded the yield strength of the rock.

An important question is whether the prestress "memory" of the rock is retained over periods of time or is only temporary. Uniaxial compression tests were conducted on several samples of Salem limestone that were all prestressed to the same level of 58 MPa. Subsequent stress cycles were performed on each sample to reestablish the prestress using the Kaiser effect after periods of 1, 3, and 60 days (fig. 13). Results showed that the rocks tested after 1, 3, and 60 days all predicted the prestress within a few percentage points. Thus, even after periods of up to 2 months, peak stress in the rock could accurately be predicted using the Kaiser effect. Another series of uniaxial compression tests was conducted on St. Cloud gray granodiorite that was prestressed to 130 MPa. Results showed that even after 150 days (5 months) the Kaiser effect was clearly present, and that peak stress could be estimated at 124 MPa, within ±9 pct of the prestressed value. For these rocks, there appears no evidence suggesting that the stress memory established by the Kaiser effect fades within short periods of time. It remains to be established whether peak stress history is retained in rock over geologic periods of time.

The Kaiser effect is known to be dependent on the confining or mean stress, at least in some rocks. Holcomb (*11*) observed that the Kaiser effect increased nearly linearly by roughly 3.4 MPa per megapascal increase in pressure in Westerly granite for the range of confining pressures from 5 to 69 MPa (10,000 psi). The Kaiser effect stress was postulated to form a damage surface, similar to the failure envelope at ultimate stress. Accordingly, for stress states below the Kaiser effect threshold, there would be no extension of damage in the rock, but those stress states reaching the damage surface would extend it (*26*). For comparison, earlier Bureau results for AE response under triaxial loading of St. Cloud gray granodiorite (*18*) were reanalyzed. Here, researchers differentiated between the "onset of emission" in those results and the abrupt change in rate of emission associated with the Kaiser effect. Cumulative AE response was determined at atmospheric pressure and confining pressures of 23, 46, and 69 MPa in conventional triaxial compression tests. The stress path first applied a uniform confining pressure to the desired test level, and then a differential stress was applied to the point where the Kaiser effect could be observed and continued through yield and failure (fig. 14). The results plotted for comparison with those of Holcomb and Costin (*26*) for the Westerly granite (fig. 15) show that the Kaiser effect "damage surface" for the St. Cloud gray granodiorite is more sensitive to confining pressure (has steeper slope). Except for the point at 46 MPa, the surface has somewhat of a linear trend and roughly parallels the failure surface (ultimate stress). The Kaiser effect increases roughly 7.9 MPa per megapascal increase in confinement. It was postulated by Holcomb (*11*) that since "ultimate failure is the result of the accumulating local failures, it would be expected that the pressure dependence of strength should be about the same as that of the Kaiser effect." Bureau results for the St. Cloud gray granodiorite tend to support that postulation; both the Kaiser effect and the ultimate stress have nearly the same dependence on confining pressure. It is further noted by Holcomb that since the Kaiser effect is influenced by all principal stresses, the total stress state may be obtainable from information locked in the core, but that the principal problem is in devising a way to separate the effects of the stress components if a unique stress state is to be determined. More research needs to be done before the Kaiser effect can be used with confidence to determine in situ stresses. However, recent preliminary studies of the Kaiser effect by Hardy (*10*) at the Pennsylvania State University suggest that triaxial stresses can be estimated with reasonable accuracy (±13 pct) using a single uniaxial test. Hardy further emphasizes that there is strong economic incentive to further develop in situ stress tests based on the Kaiser effect, since the conventional methods based on stress relief technology are considerably more expensive and time consuming. Continued research on the Kaiser effect and the development of AE pattern recognition technology therefore appears warranted.

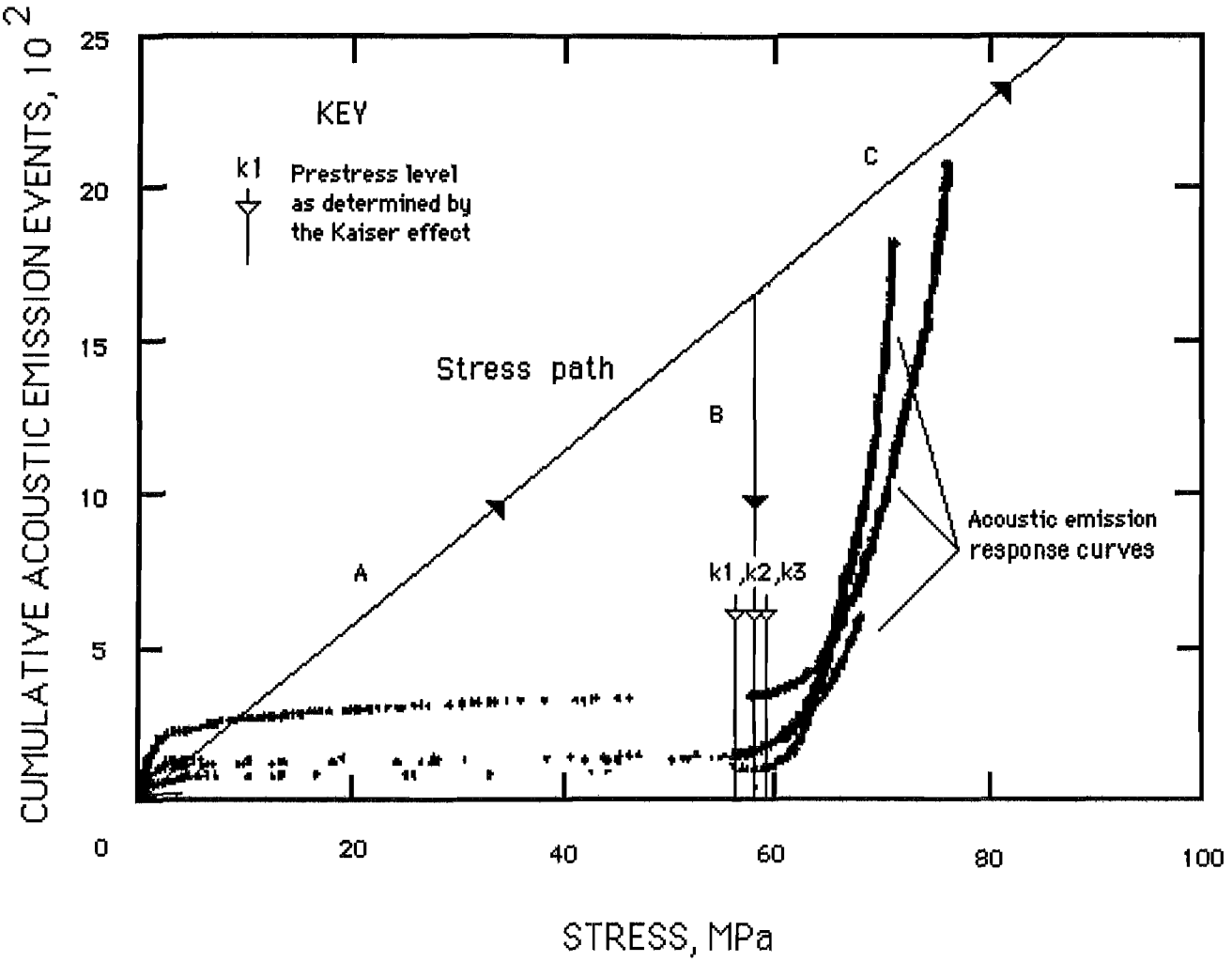

Figure 13.–Cumulative acoustic emission as a function of stress for three Salem limestone samples. Each sample was loaded to rupture under uniaxial compression at various time intervals after the initial prestress. Curve A-B represents initial stress path taken while prestress was applied. Curve A-C is stress path taken to detect Kaiser effect (for three separate samples) at time intervals of 1 (k1), 3 (k3), and 60 (k2) days following application of prestress.

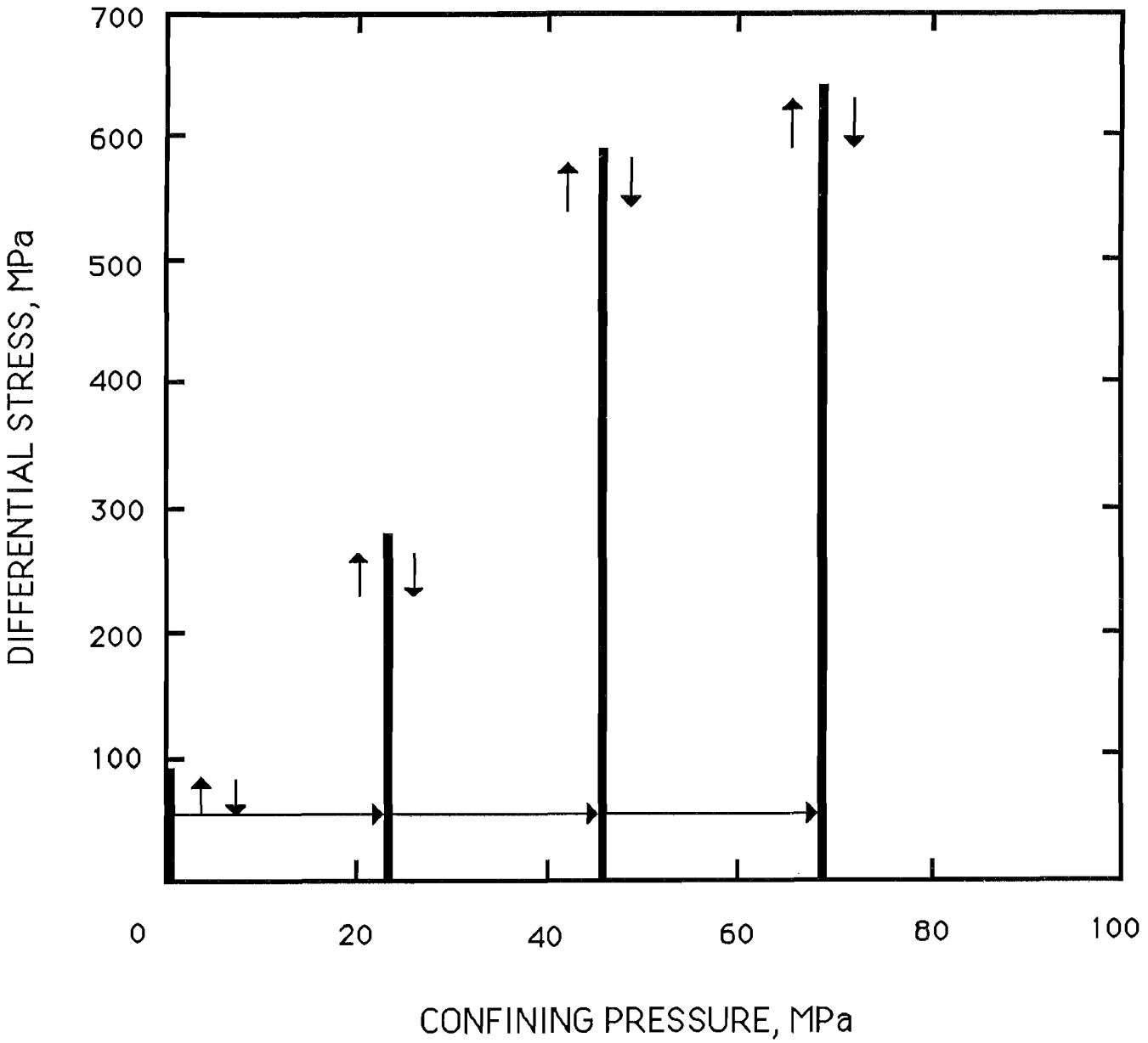

Figure 14.–Stress path used to induce damage in St. Cloud gray granodiorite sample to investigate usefulness of Kaiser effect, while sample was under triaxial compression.

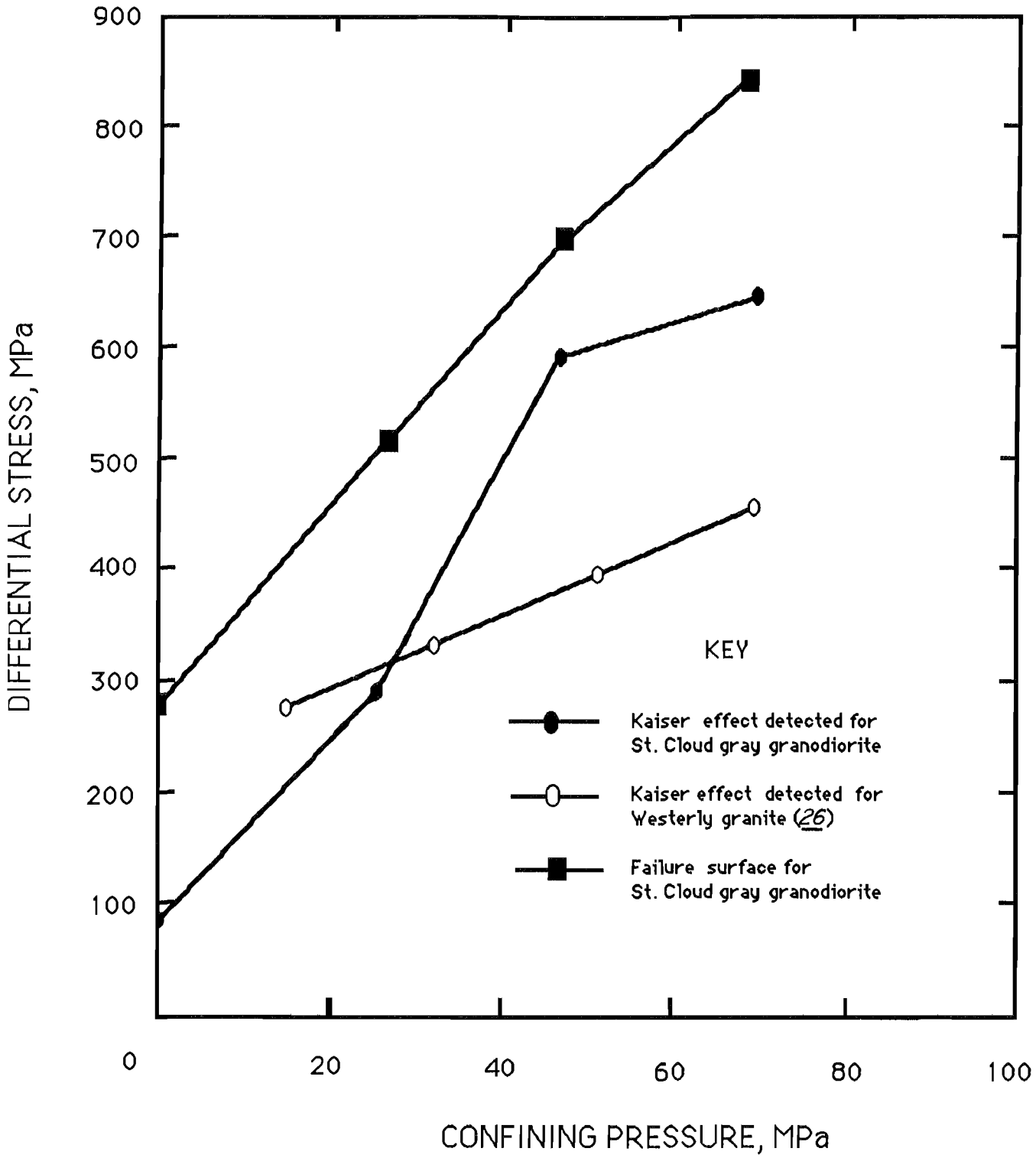

Figure 15.–Detection of peak stress levels by Kaiser effect, imposed by triaxial loading a sample of St. Cloud gray granodiorite. Results are compared with results for Westerly granite.

CONCLUSIONS

The Kaiser effect has been shown to be present and repeatable, usually within a few percentage points for several types of brittle rock. The AE response curves display repeatable signatures suggesting that pattern recognition technology can be successfully employed to interpret stress and deformation characteristics of the rock. The generalized Mogi signature (*7*), based on the shape of the cumulative response curve, displays four stages or regions, plus failure, that are diagnostic of the deformation and failure process. Although each stage was present to some extent in each of the six types of rock tested, several of the AE response curves resembled the shape variations classified by Boyce (*14*). While the latter shape variations are useful in some cases for indicating variations in rock behavior, it was found that the resultant shape of the response curve was sensitive to measurement system parameters such as the sampling rate interval and the amplitude threshold, in addition to the AE response of the rock, suggesting a need for standardization of the recording parameters. Signatures of AE within each deformation stage and captured waveforms of AE signals provide additional patterns indicative of the mechanisms of deformation and failure. These recently have been used with some success by the Canadians for indicating the level of stress in mine pillars. Stress-strain correlations for interpretation of the AE response are shown to be much more comprehensive when the volumetric stress-strain curves, rather than customary axial curves, are used for comparison. The Kaiser effect was shown to retain "memory" of peak prestresses over moderate periods of time up to 5 months. The Kaiser effect was noted to be highly sensitive to confining stresses, at least in some rocks, an item that requires further research and consideration for the interpretation of in situ field stresses. Limitations of the Kaiser effect, moreover, need to be determined in greater detail, particularly for rock that has been stressed near or beyond the yield point.

REFERENCES

1. Radcliffe, K. S., R. E. Thill, and J. A. Jessop. Use of Acoustic Velocity for Predicting Stress Under Uniaxial Compression (Pres. at 115th Annu. AIME Meet., New Orleans, LA). Soc. Min. Eng. AIME preprint 86-147, 1986, 11 pp.

2. National Research Council, Panel on Rock Mechanics Research Requirements. Rock Mechanics Research Requirements for Resource Recovery, Construction and Earthquake Hazard Reduction. Natl. Acad. Press, Washington, DC, 1981, pp. 42-66.

3. Kaiser, J. (An Investigation Into the Occurrence of Noises in Tensile Tests or a Study of Acoustic Phenomena in Tensile Tests.) Ph.D. Thesis, Tech. Hochsh. Munchen, Munich, Federal Republic of Germany, June 1964, 190 pp. (Engl. transl. from Lawrence Radiation Lab., Livermore, CA, Rep. UCRL-TRANS-1082-L).

4. Kanagawa, T., M. Hayashi, and H. Nakasa. Estimation of Geo-Stress Components in Rock Samples Using the Kaiser Effect. Cent. Res. Inst. Electr. Power Ind. (Tokyo), Rep. 375017, 1976, 26 pp.

5. Hayashi, M., T. Kanagawa, R. Hibino, S. Matojioma, and V. Tahara. Detection of Anisotropic Geostresses Trying Acoustic Emissions, and Nonlinear Rock Mechanics on Large Excavating Caverns. Paper in 4th International Congress for Rock Mechanics (Montreaux, Switzerland, Sept. 1979). A. A. Balkema, Rotterdam, Netherlands, 1979, v. 2, pp. 211-218.

6. Kurita, K., and N. Fujii. Stress Memory of Crystalline Rock in Acoustic Emission. Geophys. Res. Lett., v. 6, 1979, pp. 9-12.

7. Mogi, K. Study of the Elastic Shocks Caused by the Fracture of Heterogeneous Materials and Its Relation to Earthquake Phenomenon. Bull. Earthquake Res. Inst., Univ. Tokyo, v. 40, 1962, pp. 125-173.

8. Murayama, S. The Kaiser Effect of a Granite Under Various Loadings. Jpn. Soc. Civ. Eng., 1985, pp. 586-593.

9. Hardy, H. R., Jr., D. Zhang, and J. Zelanko. Recent Studies Relative to the Kaiser Effect in Geologic Materials. Paper in Proceedings of the 4th Conference on Acoustic Emission/Microseismic Activity in Geologic Structures and Materials (PA State Univ., Oct. 1985). Trans. Tech. Publ., Clausthal, Federal Republic of Germany, in press.

10. Hardy, H. R., Jr. Recent Geotechnical Applications of the Acoustic Emission/Microseismic Technique. Paper in Conference on Nondestructive Testing and Evaluation for Manufacturing and Construction (Univ. IL-Urbana-Champaign, Aug. 9-12, 1988). 1988, pp. 189-201; available from H. R. Hardy, Jr., PA State Univ., University Park, PA.

11. Holcomb, D. J. Using Acoustic Emission To Determine In Situ Stress: Problems and Promise. Geomechanics, v. 57, 1983, pp. 11-21.

12. Holcomb, D. J., and R. J. Martin III. Peak Stress History Using Acoustic Emissions. Paper in Research and Engineering Applications in Rock Masses, ed. by E. Ashworth (26th U.S. Symp. on Rock Mechanics, Rapid City, SD, June 26-28, 1985). A. A. Balkema, Boston, MA, 1985, pp. 715-722.

13. Holcomb, D. J., and L. S. Costin. Detecting Damage Surfaces in Brittle Materials Using Acoustic Emissions. Trans. ASME, J. Appl. Mech., v. 53, 1986, pp. 536-544.

14. Boyce, G. M., W. M. McCabe, and R. M. Koerner. Acoustic Emission Signatures of Various Rock Types in Unconfined Compression. Paper in Acoustic Emission in Geotechnical Engineering Practice. ASTM STP 750, 1981, pp. 142-154.

15. Krech, W. W., F. A. Henderson, and K. E. Hjelmstad. A Standard Rock Suite for Rapid Excavation Research. BuMlnes RI 7865, 1974, 29 pp.

16. American Society for Testing and Materials. Special Procedures for Testing Rock for Engineering Purposes. ASTM STP 479, 1970, 529 pp.

17. Brown, E. T. (ed.). Rock Characterization Testing and Monitoring–ISRM Suggested Methods. Pergamon Press, 1981, 211 pp.

18. Thill, R. E. Acoustic Methods for Monitoring Failure in Rock. Paper in New Horizons in Rock Mechanics (Proc. l4th U.S. Symp. on Rock Mechanics). Am. Soc. Civ. Eng., 1973, pp. 649-687.

19. Scholz, C. H. Experimental Study of the Fracturing Process in Brittle Rock. J. Geophys. Res., v. 73, 1968, pp. 1447-1453.

20. _____. Correction to "Experimental Study of the Fracturing Process in Brittle Rock." J. Geophys. Res., v. 73, 1968, p. 4794.

21. Brace, W. F., W. B. Paulding, Jr., and C. H. Scholz. Dilatancy in the Fracture of Brittle Rocks. J. Geophys. Res., v. 71, 1966, pp. 3939-3953.

22. Montoto, M., L. M. Suarez del Rio, A. W. Khair, and H. R. Hardy, Jr. AE in Uniaxially Loaded Granitic Rocks in Relation to Their Petrographic Character. Paper in Conference on Acoustic Emission/Microseismic Activity in Geologic Structures and Materials (PA State Univ., Oct. 1981). Trans. Tech. Publ., Clausthal, Federal Republic of Germany, 1984, pp. 83-100.

23. Lord, A. E., Jr. and R. M. Koerner. Acoustic Emissions in Geologic Materials. J. Acoust. Emiss., v. 2, No. 1, 1983, pp. 195-219.

24. Archibald, J. F., P. N. Calder, B. Moroz, T. Semadeni, and T. K. Yeo. Applications of Microseismic Monitoring to Stress and Rockburst Precursor Assessment. Min. Sci. & Techol., v. 7, 1988, pp. 123-132.

25. Kanagawa, T., M. Hayashi, and Y. Kitahara. Acoustic Emission and Overcoring Methods for Measuring Tectonic Stresses. Paper in International Symposium on Weak Rock (Tokyo, Japan, Sept. 21-24, 1981). Cent. Res. Inst. Electr. Power Ind. (Tokyo), 1981, pp. 1205-1210.

26. Holcomb, D. J. and L. S. Costin. Damage in Brittle Materials: Experimental Methods. Paper in Proceedings of the l0th U.S. National Congress of Applied Mechanics (June 16-20, 1986). ASME, 1986, pp. 107-113.